BBA - Molecular and Cell Biology of Lipids 1866 (2021) 158885

Contents lists available at ScienceDirect

BBA - Molecular and Cell Biology of Lipids

journal homepage: www.elsevier.com/locate/bbalip

Improved organotypic skin model with reduced quantity of monounsaturated ceramides by inhibiting stearoyl-CoA desaturase-1

Richard W.J. Helder [a], Jannik Rousel [a], Walter A. Boiten [a], Gerrit S. Gooris [a], Andreea Nadaban [a], Abdoelwaheb El Ghalbzouri [b], Joke A. Bouwstra [a,*]

[a] Division of BioTherapeutics, LACDR, Leiden University, Leiden, the Netherlands
[b] Department of Dermatology, LUMC, Leiden, the Netherlands

ARTICLE INFO

Keywords:
Skin
Stratum corneum
Ceramide
Stearoyl-CoA desaturase-1
Monounsaturation

ABSTRACT

Full thickness models (FTM) are 3D *in vitro* skin cultures that resemble the native human skin (NHS) to a great extent. However, the barrier function of these skin models is reduced. The skin barrier is located in the stratum corneum (SC) and consists of corneocytes embedded in a lipid matrix. In this matrix, deviations in the composition of the FTMs lipid matrix may contribute to the impaired skin barrier when compared to NHS. One of the most abundant changes in lipid composition is an increase in monounsaturated lipids for which stearoyl-CoA desaturase-1 (SCD-1) is responsible. To improve the SC lipid composition, we reduced SCD-1 activity during the generation of the FTMs. These FTMs were subsequently assessed on all major aspects, including epidermal homeostasis, lipid composition, lipid organization, and barrier functionality. We demonstrate that SCD-1 inhibition was successful and resulted in FTMs that better mimic the lipid composition of FTMs to NHS by a significant reduction in monounsaturated lipids. In conclusion, this study demonstrates an effective approach to normalize SC monounsaturated lipid concentration and may be a valuable tool in further optimizing the FTMs in future studies.

1. Introduction

Full thickness skin models (FTMs) are *in vitro* skin models that mimic native human skin (NHS) in many aspects and serve as a valuable tool to unravel biological processes in healthy and diseased skin [1]. In addition, FTMs serve as an excellent tool for the prediction of toxicity screenings and diffusion of novel compounds as an alternative for animal experiments [1–4]. However, the most important drawback is the reduced barrier function of the FTMs [5–8]. This limits the use of FTMs in the prediction of novel pharmaceutical compounds on their diffusion across the skin. Therefore, there is an urgent need for a new generation of FTMs that mimic the NHS barrier properties more closely. To improve the skin barrier of the FTMs, normalization of the stratum corneum (SC) lipid composition is considered to be crucial [9–11].

The outside-in NHS barrier is primarily located in the SC, which consists of corneocytes embedded in a lipid matrix [12]. In this lipid matrix, three main lipid classes are present: cholesterol, free fatty acids (FFAs), and ceramides (CERs). The CERs are the most complex of these lipids and over 16 subclasses have been identified [13–15]. In addition to different subclasses, each subclass has a broad distribution in their total chain length as well (sphingoid base + acyl chain) [16,17]. Although less variety in subclasses, the FFAs also have a broad distribution of chain length. Together with cholesterol, these lipids can organize themselves into two lamellar phases, the short periodicity phase (SPP) with a repeat distance of around 6 nm and the long periodicity phase (LPP) with a repeat distance of approximately 13 nm [18,19]. Within the lamellae, the lipids can adopt a very dense (orthorhombic), a less dense (hexagonal) packing or even a fluid phase. The lipid organization is depicted schematically in Fig. S1 and the molecular structure of the various CER subclasses are described in Fig. S2.

Differences in lipid composition and organization have been reported between the FTMs and NHS [16,20]. One of the most prevalent

Abbreviations: FTM, full thickness models; NHS, native human skin; SC, Stratum Corneum; CER, ceramide; saCER, saturated ceramide; muCER, monounsaturated ceramide; FFA, free fatty acid; saFFA, saturated free fatty acid; muFFA, monounsaturated free fatty acid; LPP, long periodicity phase; SPP, short periodicity phase; SCD-1, stearoyl-CoA desaturase-1.

* Corresponding author at: Einsteinweg 55, 2333 CC Leiden, Zuid-Holland, the Netherlands.
E-mail addresses: r.w.j.helder@lacdr.leidenuniv.nl (R.W.J. Helder), jrousel@chdr.nl (J. Rousel), w.a.boiten2@lacdr.leidenuniv.nl (W.A. Boiten), g.gooris@lacdr.leidenuniv.nl (G.S. Gooris), a.nadaban@lacdr.leidenuniv.nl (A. Nadaban), a.ghalbzouri@lumc.nl (A. El Ghalbzouri), Bouwstra@lacdr.leidenuniv.nl (J.A. Bouwstra).

https://doi.org/10.1016/j.bbalip.2021.158885
Received 25 October 2020; Received in revised form 24 December 2020; Accepted 8 January 2021
Available online 11 January 2021

differences is a high level of monounsaturated CERs (muCERs) and monounsaturated FFAs (muFFAs). Besides this major difference, other differences are observed as well: 1) an altered CER subclass profile, 2) a strong reduction in the FFA amount, 3) a reduction in the mean chain length (MCL) of the CERs and FFAs [5,16,21]. These changes in lipid composition lead to changes in the lipid organization. The most predominant ones include a shorter repeat distance of the LPP, the absence of the SPP and a less dense lipid packing: lipids adopt mainly a less dense hexagonal packing. Ultimately, these changes contribute to a reduced barrier function in the FTMs [16,20].

The aim in this study was to improve the lipid composition by reducing the level of muCERs and muFFAs in our in-house FTM model. This in-house model displays the alteration in lipid composition and organization as described above, such as an increase in monounsaturation of the lipids [16]. A possible underlying factor for this is the enzyme stearoyl-CoA desaturase-1 (SCD-1). Studies have reported that this enzyme is overexpressed and is also present in the suprabasal layers, whereas in NHS, SCD-1 is mainly expressed in the basal layer [16,21].

SCD-1 serves as a catalyst for creating a double bond at the Δ9 carbon in saturated FFAs (C16:0 and C18:0) to convert them in their monounsaturated counterparts (C16:1, and C18:1), respectively [22]. Subsequently, these saturated FFAs (saFFAs) and muFFAs are elongated by a group of elongases referred to as ELOVLs and finally incorporated into the SC lipid matrix [23]. Next, these (mu)FFAs are also building blocks for CERs and are linked to a sphingoid base by the group of ceramide synthases leading to the more complex CER subclasses [24–26]. However, this means that a higher quantity of both CERs and FFAs that contain monounsaturated bonds in their acyl chains are synthesized. These muCERs and muFFAs are key factors that contributes to the formation of a less dense hexagonal organization [9]. To reduce the level of monounsaturation in the SC lipids, the culture medium of our in-house developed FTM was supplemented with an SCD-1 inhibitor to normalize the lipid monounsaturation.

After generation of FTMs, the lipid composition was analyzed and a drastic reduction in the amount of muCERs and muFFAs were observed. This demonstrates that the SCD-1 inhibitor successfully inhibited the SCD-1 activity. In addition, changes were observed in the lipid synthesis, such as the increase in CER[dS] and the overall reduction in CER(EO) subclasses.

2. Materials and methods

Methods performed in this study are briefly described below. A more detailed description can be found in the Supplemental materials and methods (Supp. Methods).

2.1. Generation of the full thickness models

Prior to the SCD-1 study, two concentrations of SCD-1 inhibitor were tested: 45 nM and 450 nM. However, the 450 nM did not result in viable FTMs, therefore this study was performed with 45 nM as concentration for the SCD-1 inhibitor. To study the effects of SCD-1 inhibition, all studies were performed in triplicate using keratinocytes from three female donors (3 Caucasian female skin donors aged between 18 and 26, cell isolation is described in Supp. Methods 1). Two out of three originating NHS keratinocyte donor samples were also used as a control in the following subsequent studies (liquid-chromatography-mass spectrometry (LC-MS), quantitative polymerase chain reaction (qPCR), small angle X-ray diffraction (SAXD)). Due to limit of sample material the third control was from an additional donor. Using each donor, the FTMs were generated in triplicate. First, the dermal compartment was prepared as reported in detail previously [5,27]. To this end, rattail-collagen was populated with fibroblasts (4×10^4 fibroblasts/ml) as described before [5]. After 7 days of culturing the dermal compartment, keratinocytes (2.5×10^5 cells) were seeded onto each dermal compartment and subsequently cultured for another four days under submerged conditions. Then the FTMs were lifted to the air-liquid interface and the SCD-1 inhibitor was supplemented to the culture medium. The FTM conditions were: 1) $FTM_{CONTROL}$, that contained normal culture medium as described elsewhere [20], 2) $FTM_{SCD\text{-}1}$ that contained in addition to the normal culture medium, 45 nM of SCD-1 inhibitor AB142089 (Sigma-Aldrich, Zwijndrecht, the Netherlands) dissolved in 0.05% DMSO of the culture medium (v/v), 3) FTM_{DMSO} supplemented with 0.05% DMSO in the medium was cultured to serve as a second control. The results obtained in this study for FTM_{DMSO} and the $FTM_{CONTROL}$ were similar in all features, therefore, the FTM_{DMSO} are not shown in the Results section. The FTMs were cultured air exposed for a period of 14–17 days and medium was refreshed twice a week with freshly prepared supplements [27,28]. Subsequently, the SC was removed from the viable epidermis by trypsin digestion and used for analysis (Supp. Methods 1.1).

2.2. Analysis of the FTMs

To examine the effects of the SCD-1 inhibitor on the various characteristics of the FTMs, the following analyses were performed: immunohistochemistry (Supp. Methods 1.2), LC-MS (in Supp. Methods 1.3), qPCR (Supp. Methods 1.4), SAXD (in Supp. Methods 1.5), Fourier transformed infrared spectroscopy (FTIR, in Supp. Methods 1.6), and trans epidermal water loss (TEWL, in Supp. Methods 1.7).

2.3. Statistical analysis

Statistical analysis was performed in Graphpad 7. For statistical analysis, an unpaired *t*-test was performed between the $FTM_{CONTROL}$ and $FTM_{SCD\text{-}1}$. To compare the $FTM_{CONTROL}$ against NHS, an unpaired *t*-test was used. Significant differences are indicated by * for $p < 0.05$, ** for $p < 0.01$, and *** for $p < 0.001$.

3. Results

3.1. Supplementation of the SCD-1 inhibitor led to minor changes in the epidermal homeostasis but drastically increased SCD-1 protein expression

Before the initial study on FTMs, a small pilot was performed to determine the effects of the SCD-1 inhibitor in two different concentrations; 45 nM and 450 nM. The concentration of 45 nM is based on the reported IC50 of AB142089, which was 4.5 nM [21]. In addition to an 10 times increase, that would already demonstrate an effect without causing toxicity to the FTMs, we also wanted to include a higher concentration of the inhibitor (450 nM). This was initiated due to the high percentage of monounsaturation in the lipids of FTMs and to determine whether it would be more beneficial. However, the inhibitor concentration of 450 nM did not lead to a viable FTM (Fig. S2). Therefore, the study was performed with inhibitor SCD-1 concentration of 45 nM (referred to as the $FTM_{SCD\text{-}1}$), which was supplemented to the culture medium.

After culturing, FTMs and NHS were investigated on basal cell proliferation, early, and late differentiation by several epidermal homeostasis proteins markers (Fig. 1). Basal cell proliferation was examined by a Ki67 protein staining. As shown in Fig. 1, no significant changes in Ki67 expression was observed, irrespective the condition tested. Next, the early differentiation was investigated by staining for keratin 10 (K10) (Fig. 1). K10, which stains the suprabasal cell layers, showed no changes in expression, indicating a normal execution of the early differentiation program. Next the late differentiation protein involucrin was stained. This protein was similarly expressed in $FTM_{CONTROL}$ and $FTM_{SCD\text{-}1}$ and equally present in the stratum granulosum as well as the stratum spinosum, whereas in NHS, involucrin was restricted to the stratum granulosum (Fig. 1). When examining the SCD-1 expression, a significant difference was observed: The $FTM_{SCD\text{-}1}$ displayed a drastic increase in SCD-1 expression compared to $FTM_{CONTROL}$, but both

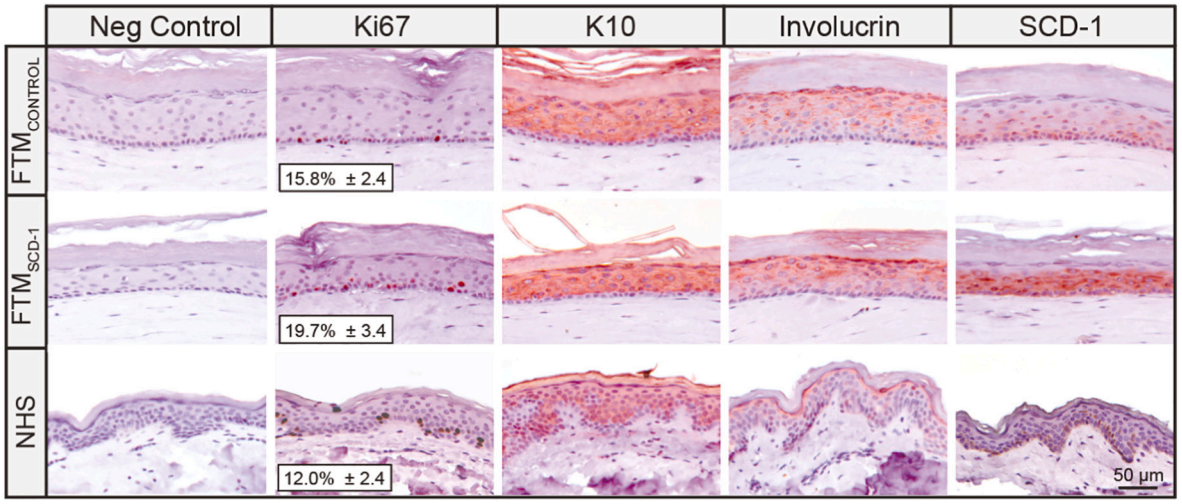

Fig. 1. Different epidermal homeostasis markers and SCD-1 were examined in FTMs and NHS. Expression of protein markers in $FTM_{CONTROL}$, FTM_{SCD-1} and NHS from left to right: negative control, proliferation (Ki67), early differentiation (K10), late differentiation (involucrin), and lipid monounsaturation enzyme SCD-1. Ki67 proliferation index determination. Scale bar: 50 µm.

displayed expression throughout the epidermis. In NHS, SCD-1 expression was less prominently present and more restricted to the basal layer (Fig. 1).

3.2. SCD-1 inhibition led to reduction of monounsaturated CER subclasses

To determine whether SCD-1 inhibition led to changes in the SC lipid composition, the CER profile in FTMs and NHS was examined. First, the extracted amount of SC lipids was determined (Fig. 2a). The amount of extracted lipids was similar between FTMs, but was significantly increased in NHS compared to the FTMs. After the lipid extraction, the peaks of all CER subclasses (saCER+muCER) in the LC-MS spectrum were integrated, processed and converted to CER amounts in nmol/mg SC (Fig. 2b). No differences in the total amount of CERs in nmol/mg SC between the FTMs and NHS were observed. Next, the absolute amounts of the CER subclasses were analyzed.

3.2.1. Quantified CER subclass composition

The individual subclasses of CER[non-EO], CER[EO], and CER[O] were plotted in absolute amounts (Fig. 2c, e, f, respectively). Individual analysis of the quantified subclasses of CER[non-EO] revealed a similar subclass profile after SCD-1 inhibition compared to $FTM_{CONTROL}$, except for an increased amount of CER[dS] subclass in FTM_{SCD-1}. Compared to NHS, in both $FTM_{CONTROL}$ and FTM_{SCD-1} an altered amount of CER [NS], [AS], [NH], [NP] and [NH] subclasses was observed. More drastic

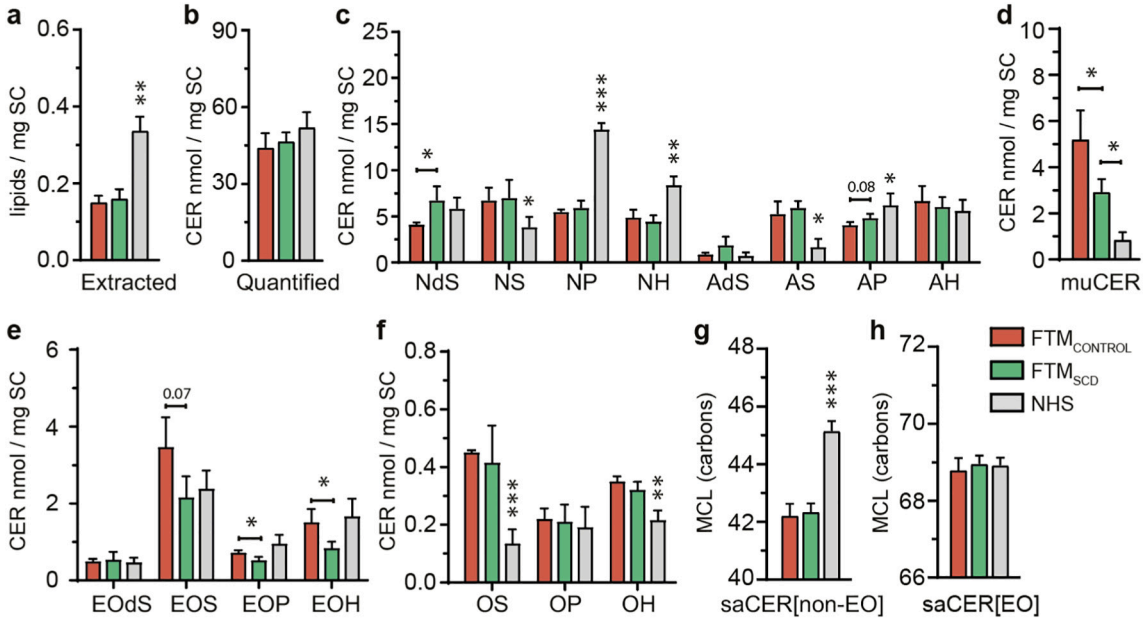

Fig. 2. SCD-1 inhibition alters lipid composition by reducing the monounsaturation, reducing the CER[EO] subclasses, and by increasing the CER[dS] fraction. During sample preparation, (a) the amount of extracted lipids was determined. (b) The total amount of CERs (saCER+muCER) in nmol/mg SC. (c) The subclasses of the CER[non-EO] (saCER+muCER). (d) The total amount of muCER[non-EO] (muCERs in nmol/mg SC). (e) Subclasses in CER[EO] (saCER+muCER). (f) Subclasses in CER[O] (saCER+muCER). The mean chain lengths for (g) saCER[non-EO] and (h) CER[EO] main peak (saCER[EO-18:2] + muCER[EO-18:1]. For statistical analysis, an unpaired *t*-test was performed between the $FTM_{CONTROL}$ and FTM_{SCD-1}. After, to compare the $FTM_{CONTROL}$ and NHS, an unpaired t-test was used. Significant differences are indicated by * for $p < 0.05$, ** for $p < 0.01$, and *** for $p < 0.001$.

changes were observed when examining the amount of muCERs after SCD-1 inhibition (Fig. 2d). This demonstrated that the SCD-1 inhibitor successfully reduced the amount of muCERs to a level more closely to that in NHS.

In addition to the CER[non-EO], the CER[EO] subclasses were also quantified (Fig. 2e). The total amount of CER[EO] was reduced in FTM_{SCD-1}, this was mainly caused by the reduction in CER[EOS] ($p = 0.07$) and a significant reduction in CER[EOP] and CER[EOH] subclasses. To study the underlying factor of this reduction, the individual monounsaturated and saturated subclasses of CER[EO] with either oleic (C18:1) or linoleic (C18:2) acid chain were analyzed (Fig. S4). This displayed that it was not one individual CER[EO] subset that was reduced, but all subsets were reduced. This reduction was most prevalent in the CER[EOS], where the combined amount of muCER[EO-18:1]/ saCER[EO-18:2] was decreased (Fig. S4a, $p = 0.06$). Similar results were observed for the muCER[EO-18:2] (Fig. S4b, $p = 0.11$) and saCER[EO-18:1] (Fig. S4c, $p = 0.07$).

Next, to determine whether the decrease in amount of CER[EO] was due to a change in the CER[O] content as these have a common synthetic pathway, the amount of CER[O] (saCER+muCER) was determined (Fig. 2f). The amount of CER[O] was similar between the FTM conditions tested. However, when studying the saCER[O] and muCER[O] composition separately (Fig. S5), an increase (but not significant) in subclasses of saCER[O] in the FTM_{SCD-1} was observed more comparable to NHS, although NHS still has significantly higher amount of saCER[O].

Another important aspect for the barrier is the mean chain length (MCL) of the lipids. This was determined for both saCER[non-EO] (Fig. 2g) and the main CER[EO] subclass (Fig. 2h) subclasses. Inhibition of SCD-1 did not have an impact on the MCL of the CER[non-EO]; The MCL was still shorter compared to that of NHS [21,29]. The MCL of CER[EO] were comparable between the FTMs and NHS groups and did not change in the FTM_{SCD-1} compared to FTM. In addition, to determine whether some CER chain lengths were more abundantly present in FTM_{SCD-1} than in FTM, the chain length distribution was determined in absolute and relative amounts (Fig. S6). The absolute chain length distribution displayed some minor but significant differences between the FTM conditions for CER[non-EO] subclasses. The amount of CERs with a chain length of C36, C38, C44 and C46 were increased in FTM_{SCD-1} compared to $FTM_{CONTROL}$. When comparing the CER chain length profile of the FTMs to NHS, there is still a large amount of CER of <C42 present in FTMs, where in NHS most CERs contain >C42. Next, the absolute CER[EO] chain length distribution was investigated. For most of the chain lengths (with the exception of C68, and C74) the chain length distribution of CER[EO] in FTM_{SCD-1} mimicked closely the distribution in NHS. However, this was mainly due to the decreased total amount of CER[EO] in FTM_{SCD-1}. When examining the relative chain length distribution, hardly no difference in chain length distribution was present between FTM_{SCD-1} and $FTM_{CONTROL}$.

3.2.2. Relative CER subclass composition

In order to relate changes in lipid composition to lipid organization, relative amounts of CER subclasses are important. The composition of the relative amounts of CER[non-EO] and CER[EO] are reported in Figs. S7 and S8, respectively. Briefly, the CER changes reported in Fig. 2 became more prominent when determining the percentage of CER subclasses. Such as the higher percentage of CER[dS] subclass and a significant reduction of most of the CER[EO] subclasses: CER[EOS], [EOH], and [EOP]. Finally, when examining the level of CER[non-EO] monounsaturation, the difference was more abundant ($p = 0.007$ *vs* $p = 0.05$) when the amount of CERs (%) was calculated for each FTM donor.

3.3. SCD-1 inhibition reduced muFFA in FTMs

3.3.1. Quantified FFA analysis

The total amount of FFA in FTMs (saFFA+muFFA) did not change upon SCD-1 inhibition (Fig. 3a). Inhibition of SCD-1 did not change the chain length distribution of saFFA either (Fig. 3b). The amount of all saFFA irrespective of their chain length was strongly reduced compared to NHS as observed in earlier studies [21,29]. Next, the muFFA profile was determined (Fig. 3c). Inhibition of SCD-1 reduced the amount of muFFA C16:1, C18:1, and C24:1 in the FTM_{SCD-1} compared to $FTM_{CONTROL}$. This was also reflected in the total amount of muFFA (Fig. 3d) and resulted in a reduced percentage of muFFA in FTM_{SCD-1}, as shown in Fig. 3e. This percentage indicates that the muFFA content in FTMs were higher than in NHS and SCD-1 inhibition was a valuable approach to reduce the muFFA content to mimic more closely the level in NHS. In addition, the FFA MCL was determined (Fig. 3f), SCD-1 inhibition did not affect the MCL.

3.3.2. Relative FFA analysis

In order to relate changes in FFA composition to lipid organization, percentages of FFA subclasses were also calculated (Fig. S9). These results demonstrate that especially long chain FFAs (>C24) were reduced and the short chain FFAs (<C22) were increased in FTMs compared to NHS. Although no significant effects were observed by SCD-1 inhibition on the MCL of the lipids, the muFFA content was significantly reduced in the FTM_{SCD-1}.

3.4. Effect of the SCD-1 inhibition on the lipid synthesis genes

To obtain information on the underlying factors that might explain the lipid composition changes after SCD-1 inhibition, several genes that are involved in lipid synthesis, elongation of FFA, and the CER synthesis were investigated (Fig. 4).

For the lipid processing genes (*SREBP-1c*, *ACC*, and *FAS*), no difference in gene expression between the FTM_{SCD-1} and $FTM_{CONTROL}$ was observed. This was also observed for the lipid elongation genes *ELOVL-1* and *ELOVL-4* (Fig. 4b). However, an increased *ELOVL-4* expression was observed in FTMs when compared to NHS. The next gene that was investigated was *SCD-1* (Fig. 4c). This gene was drastically increased in the FTM_{SCD-1} when compared to the $FTM_{CONTROL}$. $FTM_{CONTROL}$ already expressed significantly higher SCD-1 compared to NHS. To examine whether this increase was driven by *LXR* activation, *ABCA1* gene expression (Fig. 4c) was investigated. However, no change in this gene was observed, excluding LXR activation as underlying factor. Next, the CER synthesis genes were investigated. No differences in expression of the *Ceramide Synthases* (*CerS*) were observed between FTMs (Fig. 4d). However, a higher expression for *CerS2 and CerS3* were observed in FTMs compared to NHS. Finally, the gene expression of the enzymes that play a role in the head group synthesis were examined. *DES1* and *DES2* convert the CER[dS] subclass to CER[S] and CER[P], respectively. No differences were observed for these genes in $FTM_{CONTROL}$ and FTM_{SCD-1}. However, *DES2* was slightly decreased in FTMs compared to NHS.

3.5. Effect of SCD-1 inhibition on the lipid organization and TEWL

To investigate whether the changes in lipid composition affected lipid organization and subsequently SC barrier, the lipid organization and SC barrier function were examined (Fig. 5). For comparison all presented data were measured at 24 °C.

FTIR was used to determine the lateral organization of the lipids (Fig. 5a). We present the rocking vibrations at 24 °C, the temperature at which the TEWL measurement was performed (see below). The high peak intensity of the vibration located at 719 cm^{-1} together with a small shoulder located at 730 cm^{-1} in the FTIR spectrum of $FTM_{CONTROL}$ indicates that most lipids adopt a hexagonal packing. A similar rocking pattern was observed for FTM_{SCD-1}. In the spectrum of NHS, the intensity of the vibrations at 730 cm^{-1} was much stronger indicating that a higher fraction of lipids adopt to an orthorhombic organization. This demonstrates a less dense lipid organization in the FTMs compared to that in NHS.

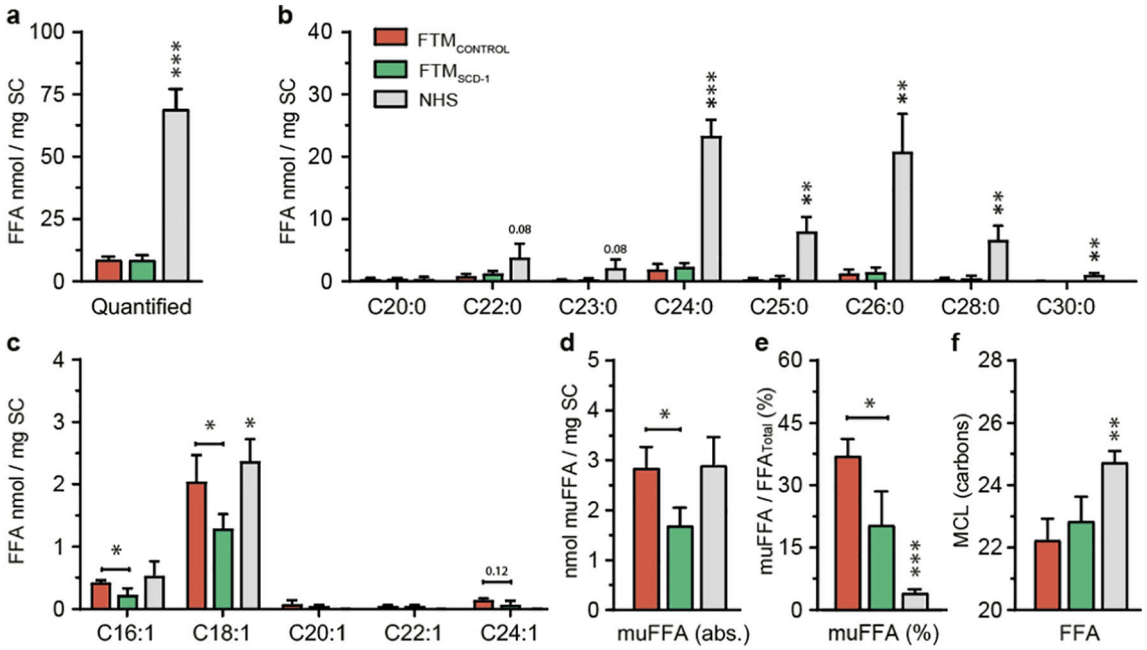

Fig. 3. SCD-1 inhibition led to a reduction in the amount of monounsaturated FFAs. (a) Amount of FFA in nMol/mg SC (b) Absolute saFFAs as function of chain length; (c) Absolute amount of muFFAs as function of chain length; (d) Absolute amount of muFFA in nmol/mg SC; (e) The percentage of muFFA; (f) the saFFA MCL. For statistical analysis, an unpaired *t*-test was performed between the FTM$_{CONTROL}$ and FTM$_{SCD-1}$. To determine whether significant differences were observed between FTM$_{CONTROL}$ and NHS, an unpaired t-test was used. Significant differences are indicated by * for $p < 0.05$, ** for $p < 0.01$, and *** for $p < 0.001$.

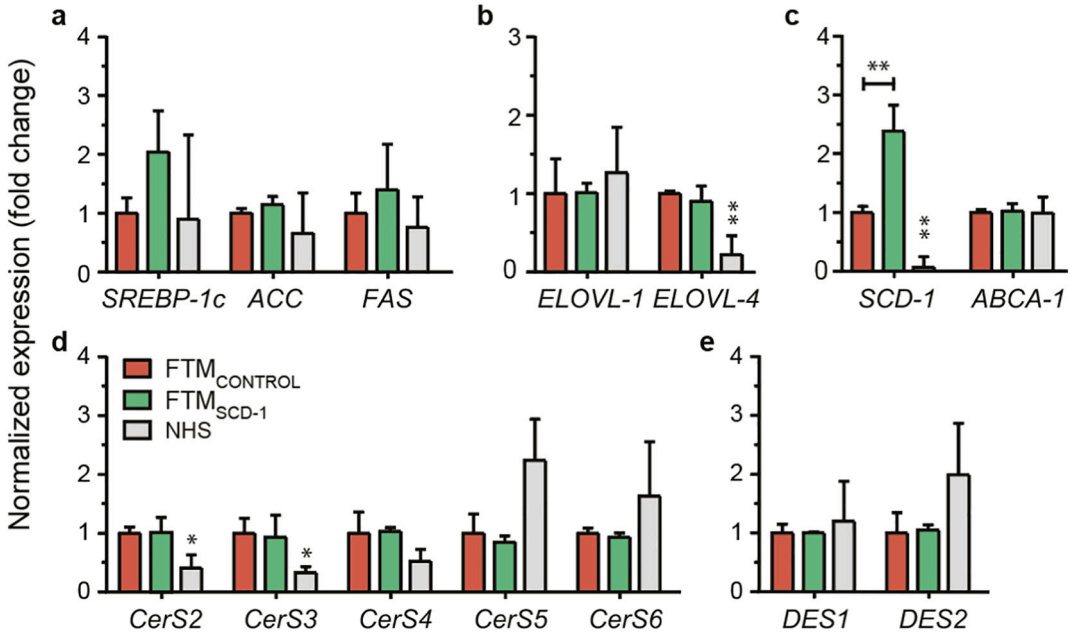

Fig. 4. Minor changes in the expression of genes involved in lipid synthesis, lipid processing, or CER synthesis after SCD-1 inhibition. Lipid synthesis genes investigated for FTM$_{CONTROL}$, FTM$_{SCD-1}$, and NHS. (a) Lipid synthesis genes *SREBP-1c*, *ACC*, and *FAS*. (b) Lipid elongases *ELOVL-1* and *ELOVL-4*. (c) Lipid desaturase *SCD-1* and *LXR* downstream target *ABCA1*. (d) *CER synthases 2–6*, and (e) CER processing enzymes *DES1* and *DES2*. For statistical analysis, an unpaired *t*-test was performed between the FTM$_{CONTROL}$ and FTM$_{SCD-1}$. To compare the FTM$_{CONTROL}$ and NHS, an unpaired t-test was used. Significant differences are indicated by * for $p < 0.05$, ** for $p < 0.01$.

Next, we determined the lamellar organization using X-ray diffraction (Fig. 5), the peak positions, indicated by I, II and III refer to the various orders of a lamellar phase with a repeat distance of 12.1 nm and 12.2 nm for the FTM$_{SCD-1}$ and FTM$_{CONTROL}$, respectively. Besides this diffraction pattern two additional small peaks were observed in the SAXD profile, indicated by + and #.

To determine whether the changes in lipid organization (FTIR and SAXD) led to a change in the barrier function of FTM$_{SCD-1}$ compared to FTM$_{CONTROL}$ the TEWL was measured for FTMs and NHS (Fig. 5c). No differences were observed after SCD-1 inhibition in the FTMs. However, the TEWL of NHS was approximately 4.5 times lower than that of the FTM$_{CONTROL}$.

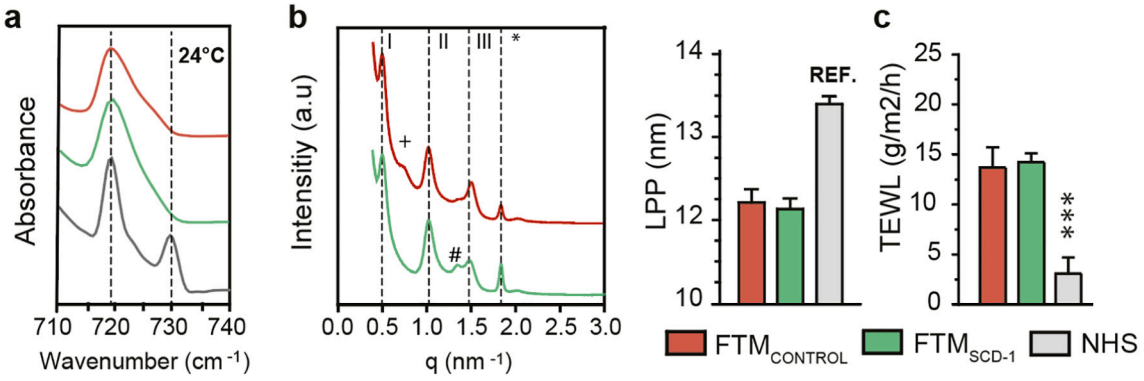

Fig. 5. SCD-1 inhibition does not change lipid organizations or lipid permeation. The lipid organization was analyzed for the FTMs and NHS at 24 °C (a) the lateral organization by displaying the rocking region and (b) X-ray diffraction profile for FTMs and the LPP repeat distance. Diffraction order of the LPP is indicated by I, II, and III. The cholesterol phase is indicated by the asterix (*). Unknown phases are indicated by + and #. The repeat distance is provided in the bar plot, with NHS as a reference [18]. (c) The TEWL values are plotted in a barplot. For statistical analysis, an unpaired *t*-test was performed between the $FTM_{CONTROL}$ and FTM_{SCD-1}. After, to compare the $FTM_{CONTROL}$ *vs* NHS, an unpaired t-test was used. Significant differences are indicated by *** for $p < 0.001$.

4. Discussion

Our aim was to improve the lipid composition and organization in the FTM model by modulating the activity of SCD-1. By inhibiting SCD-1, several modifications were observed on the lipid composition. The most important modification was the reduction in the amount of muCERs and muFFAs in the SC of the FTM_{SCD-1}, which resembles the lipid composition in NHS more closely. Another important finding was that the quantity of lipids remained similar after SCD-1 inhibition, which indicates that the total amount of lipids synthesized was unaffected by the SCD-1 inhibition and thus the synthesis of saCERs and saFFAs was increased at the expense of the monounsaturated variant. In addition, several other lipid compositional changes were observed.

First, there was a strong decrease in the amount of CER[EO] observed in the FTM_{SCD-1}. Interestingly, when displaying the individual CER[EO] subsets, both muCER[EO-18:2] and saCER[EO-18:1] are reduced, together with the main CER[EO] peak composed of two CER subclasses: muCER[EO-18:1]/saCER[EO-18:2]. This reveals that not only the muCER[EO] contributed to this reduction, but the CER[EO-18:1] as well. To understand why the CER[EO] was reduced, as a first possible underlying factor, enzymes responsible for the synthesis of CER [EO] were investigated. For this synthesis CerS3 and ELOVL4 are required [30], but the gene level for *ELOVL4* and *CerS3* did not change between $FTM_{CONTROL}$ and FTM_{SCD-1}. A second possible factor is an increase in CER[O], since CER[EO] is a precursor for CER[O] [31,32]. However, similar amounts of CER[O] were observed in the FTMs. A third explanation is a reduction in the amount of oleic acid (C18:1) for the synthesis of the CER[EO-18:1]. The amount of C18:1 was reduced in the FTM_{SCD-1} and therefore might be an underlying factor of the reduction of CER[EO-18:1]. When comparing FTMs to NHS, the amount of CER[EO] in FTMs is increased. Both *CerS3* and *ELOVL4* are known to play a key role in the synthesis of CER [4,30], the increased mRNA expression of these genes in FTMs might explain why the amount of CER [EO] is higher in FTMs.

Second, we observed an increase in the absolute amount of CER[dS] in the FTM_{SCD-1} compared to the $FTM_{CONTROL}$. This effect was even more prevalent when relative amounts of CERs were calculated. To investigate whether the increase in the amount of CER[dS] was due to a reduction in the CER head group synthesis genes, the CER subclass synthases *DES1* and *DES2* that are responsible for the conversion of CER [dS] to CER[S] and CER[P], respectively, were investigated on gene level. As both FTMs had similar mRNA level for *DES1* and *DES2*, there is no indication that these genes are an underlying factor of the shift towards more CER[dS]. However, when observing the morphology of the FTM_{SCD-1}, the epidermis does appear thinner. Perhaps, the differentiation is performed more rapidly, giving the ceramide processing enzymes less time to convert the head groups resulting in a higher level of CER[dS]. In addition, higher levels of CER[dS] were also observed in mouse skin, which also has a very thin epidermis [33]. Indicating that the thickness of the epidermis might have an impact on the subclasses.

When studying epidermal morphology and protein expression, an interesting observation is that SCD-1 inhibition resulted in a drastic increase in SCD-1 expression on both protein and RNA level. Even with an increased expression, the SCD-1 inhibitor still inhibited the majority of the protein, since there was a significant reduction in muCERs observed. This increase in SCD-1 protein level was likely due to the necessity to maintain several crucial biological processes, such as regulating cell survival, membrane integrity, or preventing lipotoxity in the cells [34–38].

Although the effects of SCD-1 inhibiting resulted in an improved lipid composition, the observed changes ultimately did not lead to alterations in the lateral organization and both FTMs adopted a hexagonal lipid organization. In order to advance the lipid organization of FTMs, several key-changes may be an important next step to generate FTMs with normalized barrier function: 1) Perhaps the most crucial change, is the increase in the quantity of FFAs. In NHS, the ratio between CER:FFA in this study is approximately 0.8:1, whereas the ratio in FTMs is approximately 1:0.125. Normalization of this ratio would promote the lipids to adopt an orthorhombic packing in FTMs [39]. 2) An increase in the MCL of both CERs and FFAs would enhance SC lipids to adopt an orthorhombic organization [21]. Another study demonstrated that LXR inhibition reduced the muCERs, but at the same time also an increase in chain length was observed [21]. This subsequently also led to an improved lipid organization, demonstrating the importance of targeting both the monounsaturation and lipid chain length. 3) A further reduction in the amount of muCERs and muFFAs would likely result in a higher fraction of lipids forming an orthorhombic organization as shown in previous studies [9].

SCD-1 inhibition did not alter the lamellar organization. The diffraction patterns of the FTMs revealed lamellar phases in the FTMs. Although it remains to be elucidated why the phases + and # formed, these small changes are most probably observed due to the CER subclass composition as this composition is crucial for the formation of the lamellar phases [40]. In the FTM_{SCD-1}, the fraction of CER[EO] is reduced and the additional phase + is no longer present, which could indicate that the abundant presence of CER[EO] contributes to this peak as suggested in previous studies [41]. The phase # might be attributed to the increased amounts of CER[dS] in the FTM_{SCD-1}, since the $FTM_{CONTROL}$ does not contain this phase.

To conclude, this study demonstrates that SCD-1 activity could be successfully reduced and that SCD-1 modulation can be a tool to lower the amount of muCERs and muFFAs in our FTM models. However, although a reduced SCD-1 activity improved the lipid composition, it did not result in an improved barrier function. This demonstrates the complexity of the lipid synthesis and the subsequent formation of the lipid organization. Nevertheless, it is important to know that the approach to reduce the monounsaturated lipids is useful, it should be combined with other targeted approaches to improve the lipid composition in order to generate the next generation of FTMs that even better mimic NHS.

CRediT authorship contribution statement

Richard W.J. Helder: Conceptualization, Methodology, Resources, Investigation, Formal analysis, Visualization, Writing – original draft, Writing – review & editing. **Jannik Rousel:** Methodology, Resources, Investigation, Formal analysis. **Walter A. Boiten:** Software, Formal analysis. **Gerrit S. Gooris:** Software, Formal analysis. **Andreea Nadaban:** Formal analysis. **Abdoelwaheb El Ghalbzouri:** Conceptualization, Methodology, Supervision, Project administration, Funding acquisition, Writing – review & editing. **Joke A. Bouwstra:** Conceptualization, Methodology, Supervision, Project administration, Funding acquisition, Writing – review & editing.

Declaration of competing interest

The authors declare that they have no known competing financial interests or personal relationships that could have appeared to influence the work reported in this paper.

Acknowledgements

We would like to thank the Dutch Technology Foundation TTW for their grand contribution (13151). TTW is also part of the Netherlands Organization for Scientific Research (NWO). We thank Evonik for their supply of ceramides. Last, we like to thank the DUBBLE beam line staff of station BM26 for their support and help the European synchrotron radiation facility (Grenoble, France).

Appendix A. Supplementary data

Supplementary data to this article can be found online at https://doi.org/10.1016/j.bbalip.2021.158885.

References

[1] H. Niehues, et al., 3D skin models for 3R research: the potential of 3D reconstructed skin models to study skin barrier function, Exp. Dermatol. 27 (5) (2018) 501–511.
[2] A. El Ghalbzouri, et al., Leiden reconstructed human epidermal model as a tool for the evaluation of the skin corrosion and irritation potential according to the ECVAM guidelines, Toxicol. in Vitro 22 (5) (2008) 1311–1320.
[3] W. Lilienblum, et al., Alternative methods to safety studies in experimental animals: role in the risk assessment of chemicals under the new European Chemicals Legislation (REACH), Arch. Toxicol. 82 (4) (2008) 211–236.
[4] M. Schäfer-Korting, et al., The use of reconstructed human epidermis for skin absorption testing: results of the validation study, Alternatives to Laboratory Animals: ATLA 36 (2) (2008) 161–187.
[5] V.S. Thakoersing, et al., Unraveling barrier properties of three different in-house human skin equivalents, Tissue Eng Part C Methods. 18 (1) (2012) 1–11.
[6] M. Schäfer-Korting, et al., Reconstructed human epidermis for skin absorption testing: results of the German prevalidation study, Altern. Lab. Anim 34 (2006) 283–294.
[7] M. , V.G., et al., Three-dimensional skin models as tools for transdermal drug delivery: challenges and limitations. Expert Opin Drug Deliv., 2011 8(6): p. 705–20.
[8] G.E. Flaten, et al., In vitro skin models as a tool in optimization of drug formulation, Eur. J. Pharm. Sci. 30 (75) (2015) 10–24.
[9] E.H. Mojumdar, et al., Monounsaturated fatty acids reduce the barrier of stratum corneum lipid membranes by enhancing the formation of a hexagonal lateral packing, Langmuir. 30 (22) (2014) 6534–6543.
[10] J. van Smeden, et al., The importance of free fatty acid chain length for the skin barrier function in atopic eczema patients, Exp. Dermatol. 23 (1) (2014) 45–52.
[11] J., V.S. and J.A. Bouwstra, Stratum corneum lipids: their role for the skin barrier function in healthy subjects and atopic dermatitis patients. Curr Probl Dermatol., 2016. 49: p. 8–26.
[12] E. Proksch, J.M. Brandner, J.M. Jensen, The skin: an indispensable barrier, Exp. Dermatol. 17 (12) (2008) 1063–1072.
[13] S. Motta, et al., Ceramide composition of the psoriatic scale, Biochim. Biophys. Acta 1182 (2) (1993) 147–151.
[14] W. Boiten, et al., Quantitative analysis of ceramides using a novel lipidomics approach with three dimensional response modelling, Biochimica et Biophysica Acta (BBA) - Molecular and Cell Biology of Lipids 1861 (11) (2016) 1652–1661.
[15] R. t'Kindt, et al., Profiling and characterizing skin ceramides using reversed-phase liquid chromatography–quadrupole time-of-flight mass spectrometry, Anal. Chem. 84 (1) (2012) 403–411.
[16] V.S. Thakoersing, et al., Increased presence of monounsaturated fatty acids in the stratum corneum of human skin equivalents, J. Investig. Dermatol. 133 (1) (2013) 59–67.
[17] J. van Smeden, et al., LC/MS analysis of stratum corneum lipids: ceramide profiling and discovery, J. Lipid Res. 52 (6) (2011) 1211–1221.
[18] J.A. Bouwstra, et al., Structural investigations of human stratum corneum by small-angle X-ray scattering, J Invest Dermatol (6) (1991) 1005–1012.
[19] M. Boncheva, The physical chemistry of the stratum corneum lipids, Int. J. Cosmet. Sci. 36 (6) (2014) 505–515.
[20] V.S. Thakoersing, et al., Unraveling barrier properties of three different in-house human skin equivalents, Tissue Engineering Part C: Methods 18 (1) (2011) 1–11.
[21] R.W.J. Helder, et al., The effects of LXR agonist T0901317 and LXR antagonist GSK2033 on morphogenesis and lipid properties in full thickness skin models, Biochim. Biophys. Acta Mol. Cell Biol. Lipids 1865 (2019).
[22] C.M. Paton, J.M. Ntambi, Biochemical and physiological function of stearoyl-CoA desaturase, Am. J. Physiol. Endocrinol. Metab. 297 (1) (2009) E28–E37.
[23] M. Rabionet, K. Gorgas, R. Sandhoff, Ceramide synthesis in the epidermis, Biochim. Biophys. Acta 1841 (3) (2014) 422–434.
[24] A. Kihara, Synthesis and degradation pathways, functions, and pathology of ceramides and epidermal acylceramides, Prog. Lipid Res. 63 (2016) 50–69.
[25] Y. Mizutani, et al., Ceramide biosynthesis in keratinocyte and its role in skin function, Biochimie 91 (2009) 784–790.
[26] Y. Masukawa, et al., Comprehensive quantification of ceramide species in human stratum corneum, J. Lipid Res. 50 (8) (2009) 1708–1719.
[27] V. van Drongelen, et al., Barrier properties of an N/TERT-based human skin equivalent, Tissue Eng Part A. 20 (21−22) (2014) 3041–3049.
[28] M. Ponec, et al., The formation of competent barrier lipids in reconstructed human epidermis requires the presence of vitamin C, J Invest Dermatol. 109 (3) (1997) 348–355.
[29] Helder, R.W.J., et al., Contribution of palmitic acid to epidermal morphogenesis and lipid barrier formation in human skin equivalents. Int J Mol Sci., 2019. 20(23).
[30] Y. Mizutani, et al., Cooperative synthesis of ultra long-chain fatty acid and ceramide during keratinocyte differentiation, PLoS One 8 (2013).
[31] Y. Zheng, et al., Lipoxygenases mediate the effect of essential fatty acid in skin barrier formation: a proposed role in releasing omega-hydroxyceramide for construction of the corneocyte lipid envelope, J. Biol. Chem. 286 (27) (2011) 24046–24056.
[32] P. Krieg, G. Fürstenberger, The role of lipoxygenases in epidermis, Biochim. Biophys. Acta 1841 (2014) 390–400.
[33] R. Martins Cardoso, et al., Barrier lipid composition and response to plasma lipids: a direct comparison of mouse dorsal back and ear skin, Exp Dermatol (2020) 548–555.
[34] M. Miyazaki, W.C. Man, J.M. Ntambi, Targeted disruption of stearoyl-CoA desaturase1 gene in mice causes atrophy of sebaceous and meibomian glands and depletion of wax esters in the eyelid, J. Nutr. 131 (2001) 2260–2268.
[35] S. Jackowski, Cell cycle regulation of membrane phospholipid metabolism, J. Biol. Chem. 1271 (1996) 20219–20222.
[36] H. Sampath, et al., Skin-specific deletion of stearoyl-CoA desaturase-1 alters skin lipid composition and protects mice from high fat diet-induced obesity, J. Biol. Chem. 284 (30) (2009) 19961–19973.
[37] L.S. Golfman, M. Bakovic, D.E. Vance, Transcription of the CTP: phosphocholine cytidylyltransferase alpha gene is enhanced during the S phase of the cell cycle, J. Biol. Chem. 276 (2001) 43688–43692.
[38] L.O. Li, E.L. Klett, R.A. Coleman, Acyl-CoA synthesis, lipid metabolism and lipotoxicity, Biochim. Biophys. Acta 1801 (2010) 246–251.
[39] J.A. Bouwstra, et al., Phase behavior of lipid mixtures based on human ceramides: coexistence of crystalline and liquid phases, J. Lipid Res. 42 (2001) 1759–1770.
[40] J.v. Smeden, et al., The important role of stratum corneum lipids for the cutaneous barrier function, Biochim Biophys Acta 1841 (2014) 295–313.
[41] D. Groen, G.S. Gooris, J.A. Bouwstra, Model membranes prepared with ceramide EOS, cholesterol and free fatty acids form a very unique lamellar phase, Langmuir 26 (2010) 4168–4175.